ChemComm
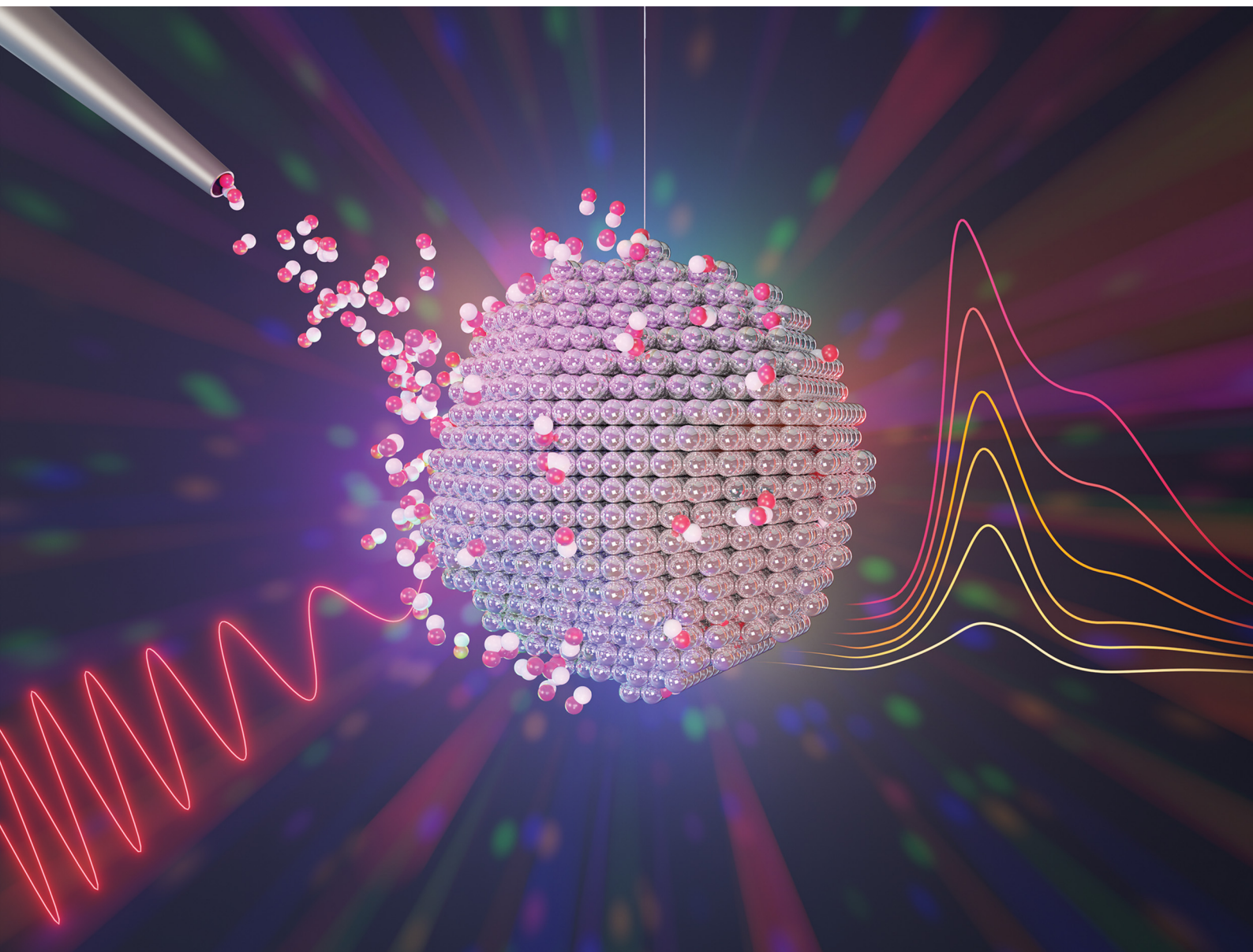
Chemical Communications

rsc.li/chemcomm

COMMUNICATION
Christian Reece *et al.*
Using precise gas exposures to resolve surface site filling in
diffuse reflectance infrared Fourier transform spectroscopy
(DRIFTS)

COMMUNICATION

Check for updates

Using precise gas exposures to resolve surface site filling in diffuse reflectance infrared Fourier transform spectroscopy (DRIFTS)†

Audrey Dannar, [‡][a] Hadley Nunn,[‡][ab] Christopher R. O'Connor [a] and Christian Reece *[a]

In this communication we report how to assemble a DRIFTS system that can precisely control the pressure in the cell from $<10^{-6}$ Torr to atmospheric pressure using easily accessible components. As a proof-of-principle we adsorb and react CO over a Pd/Al$_2$O$_3$ catalyst where we can observe pressure, temperature, and reaction-dependent preferential binding to adsorption sites.

Infrared (IR) spectroscopy is one of the most popular techniques for characterising materials due to its accessibility and versatility. In particular, diffuse reflectance Fourier transform IR spectroscopy (DRIFTS) has been used extensively to characterise the structure and reactivity of heterogeneous catalysts.[1,2] Structural insight can be inferred from the vibrational frequencies of a probe molecule (*e.g.*, CO or NH$_3$) adsorbed on the catalyst surface and mechanistic insight can be obtained by recording spectra *in situ* to determine what reaction intermediates are present. In both cases the observed frequencies are often benchmarked against experimental measurements performed using ultra-high vacuum (UHV) Reflectance-absorbance IR spectroscopy (RAIRS) over planar model systems,[3] or against theoretical simulations using density functional theory. The ability to precisely control both the structure and the environment in UHV RAIRS is critical to deconvolute fine structural details and accurately resolve surface species over a range of coverages and temperatures. However, for technical catalysts (*e.g.*, metal nanoparticles supported on metal oxides), which tend to be investigated under elevated temperatures and pressures using DRIFTS, the assignment of vibrational frequencies is non-trivial due to the increased environmental and structural complexity, particularly in cases where the reaction intermediates and structural features are unknown,

or where vibrational features overlap. In this communication, we provide a design for a DRIFTS system capable of precisely controlling the gas environment from $<10^{-6}$ torr to atmospheric pressure. While FTIR measurements over powdered samples at pressures as low as UHV have been performed previously, they require complex, bespoke vacuum systems.[4,5] The system design outlined in this work uses standardised and readily accessible components meaning it can be easily implemented in most DRIFTS setups and is compatible with most standard probe molecules. Using precise CO exposures, we measure CO adsorption and oxidation over a Pd/Al$_2$O$_3$ catalyst as a proof-of-principle. We observe the preferential filling of surface sites that is dependent on both temperature and initial surface state. With controlled gas exposures and thus longer timeframes to saturation, our measurements achieve a feature resolution unavailable at higher pressures alone. While this work focuses on the application to powder catalysts, this technique is applicable to a wide range of materials beyond catalysts, providing a tool for the elucidation of previously obscured fine structural details that affect material performance.

The vacuum DRIFTS system outlined in this work was assembled using entirely commercially available components and can easily be coupled with existing UHV systems. While the setup can be made compatible with a variety of cells and spectrometers, we utilise a DRIFTS cell capable of temperature measurements from -150 to $600\ ^\circ$C (Harrick Scientific, CHC-CHA-5). A schematic outlining the DRIFTS setup is shown in Fig. 1, and a photograph of the system shown in Fig. S1 (ESI†). The gas flow is controlled using a home-built transient flow system, which has previously been described previously,[6] but a traditional gas flow setup is also sufficient. The inlet of the DRIFTS cell is a 1/4″ VCO fitting that is connected to a manual 3-way ball valve (Fig. 1 valve 1, Swagelok, SS-42GXS4) that can select between an atmospheric pressure gas flow line or a UHV variable leak valve (Duniway, VLVE-1000) that is connected *via* a 1/4″ Swagelok to a DN40CF adaptor (Kurt J Lesker, F0275X4SWG). The gas behind the leak valve is controlled
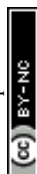
*[a] Rowland Institute at Harvard, Harvard University, Cambridge, MA, USA.
E-mail: christianreece@fas.harvard.edu*
[b] Department of Chemistry, Tufts University, Medford, MA, USA

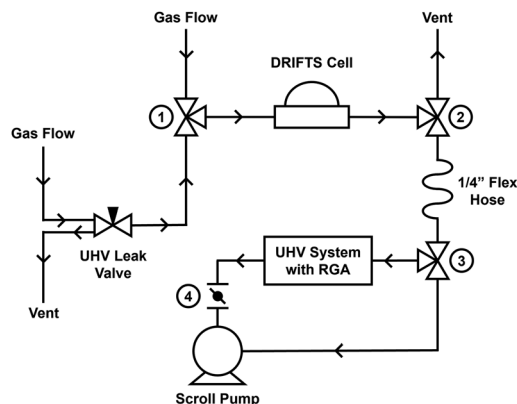† Electronic supplementary information (ESI) available. See DOI: https://doi.org/10.1039/d5cc03213j
‡ These authors contributed equally.

Fig. 1 Schematic diagram outlining the design of the vacuum DRIFTS system.

Fig. 2 DRIFT spectra showing CO adsorption over a 5% Pd/Al$_2$O$_3$ catalyst as a function of CO partial pressure in the DRIFTS cell at (a) 85 °C, and (b) −93 °C.

using the gas flow system that is connected *via* two 1/8″ Swagelok to DN16CF fitting adapters for the inlet and outlet. The outlet of the DRIFTS cell is a 1/4″ VCO fitting that is connected to a manual 3-way ball valve (Fig. 1 valve 2, Swagelok, SS-42GXS4) that selects between a ventilation line and a 2′ long 1/4″ stainless steel flex hose (Swagelok, SS-FL4TA4TA4) that is connected to another 3-way ball valve (Fig. 1 valve 3, Swagelok, SS-42GXS4) that can select between a line that connects to a roughing scroll pump (Edwards nXDS6iC) or UHV system that contains a turbomolecular pump (Edwards nEXT85D) *via* a side ported zero length DN40CF flange (IdealVac, P1011289). The setup of the DRIFTS system allows for operation under atmospheric pressure flow and vacuum conditions and utilises the same scroll pump for backing the UHV pumping system as for when rough pumping on the DRIFTS system. Because of this a valve (Fig. 1, valve 4) must be installed to allow for isolation of the two pumping systems to prevent possible backstreaming into the turbo pump when switching between atmospheric and vacuum DRIFTS. The base pressure of the UHV system when connected to the DRIFTS cell is read *via* a wide range gauge (Edwards WRG-S-DN40CF) and is typically <1 × 10⁻⁸ Torr, which corresponds to a base pressure of ∼1 × 10⁻⁶ Torr in the DRIFTS cell (see Section S1, ESI†).

To perform vacuum DRIFTS, the UHV variable leak valve and valve 3 are both closed and the UHV system is isolated from the scroll pump by closing valve 4 (IdealVac, P104243). Valves 1 and 2 are then opened to the leak valve and the 1/4″ flex hose, respectively. Valve 3 is slowly opened to the scroll pump, allowing the scroll pump to evacuate the system up to the leak valve. Caution should be taken as it is easy to disturb the catalyst bed during this step. Once the pressure of the system stabilises, valve 4 is reopened and valve 3 can be slowly opened to the UHV system to allow the entire system up to the leak valve to be evacuated. The pressure in the DRIFTS cell can then be controlled by dosing gas using the leak valve. To switch the system back to atmospheric flow mode, valve 2 is closed to isolate the pumping system from the DRIFTS cell and inert gas is flowed for a few minutes through the leak valve to re-pressurize the cell, and then the leak valve is closed. Valve 1
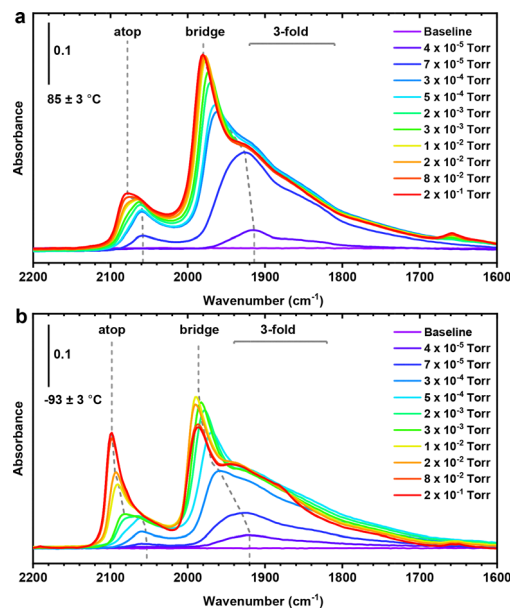
can then be switched to the gas flow system that is set to a low flow rate of inert gas, after which valve 2 can be opened to the ventilation line without exposing the system to air. As it is not possible to directly record the pressure in the DRIFTS cell, the pressure was calibrated using a test cell of comparable volume to the DRIFTS cell, with the pressure in the cell determined using the following relationship $P_{cell} = 233.3 \times P_{system}^{0.83}$ (see Section S1, ESI†). We observe a ∼10³ Torr offset between the pressure in the UHV system, and the pressure observed in the DRIFTS cell.

As a proof-of-principle, we report CO adsorption over 15 mg of a standard Pd/Al$_2$O$_3$ catalyst (5% Pd/Al$_2$O$_3$, ESCAT™ 1241) under CO pressures ranging from 10⁻⁵ Torr to 10⁻¹ Torr at liquid nitrogen cooled (−93 °C) and elevated (85 °C) temperatures to showcase how vacuum DRIFTS can measure the preferential filling of surface sites under different conditions (Fig. 2). For experimental information see Sections S2 and S3 (ESI†). The preferential binding of CO was measured by slowly opening the leak valve and allowing the surface to saturate under a series of stabilised CO pressures.

Fig. 2 shows steady-state CO DRIFT spectra of Pd/Al$_2$O$_3$ at the indicated CO pressures while held at 85 °C and −93 °C, respectively. In both experiments the temperatures drifted by ±3 °C. At cryogenic temperatures, temperature can decrease when increasing pressure due to increased thermal conductivity. To mitigate these decreases, the heater in the DRIFTS cell was used to compensate and restabilise the temperature before continuing the experiment. Generally, the Pd/Al$_2$O$_3$ surface adsorbs CO in atop (2050–2100 cm⁻¹), bridge (1990–1850 cm⁻¹), and three-fold (∼1850 cm⁻¹) sites similar to other reported measurements over supported Pd catalysts.[7,8] Our data is also in relatively good agreement with RAIRS data of

ChemComm

Pd(111) that reveals peaks assigned to atop CO ($\sim$2110 cm^{-1}) and three-fold CO ($\sim$1895 cm^{-1}) when exposed to 1×10^{-6} Torr CO at very low temperatures ($\sim$−120 °C),[9] and PM-RAIRS data of Pd(111) that exhibits a peak at 1990 cm^{-1} that is associated with bridge-bound CO when exposed to 600 mbar CO.[10] It's important to note that the assignment of absorbance features is non-trivial, but where possible, it is discussed below with the peak assignments outlined in Section S4 and Tables S1, S2 (ESI†).

At elevated temperatures (85 °C, Fig. 2a) when the Pd/Al$_2$O$_3$ catalyst is exposed to a CO pressure of 4×10^{-5} Torr two broad yet distinct peaks at $\sim$1925 cm^{-1} and $\sim$1850 cm^{-1} are observed that are assigned to CO in bridge and three-fold sites, respectively.[11] When the pressure is increased to 7×10^{-5} Torr a peak at $\sim$2060 cm^{-1} appears, that is related to atop CO. When the pressure is increased to 3×10^{-4} Torr, the peak at $\sim$1850 cm^{-1} related to the three-fold hollow sites reaches is maximum magnitude, suggesting that the sites are saturated at this pressure. Simultaneously, a new peak emerges at 1960 cm^{-1} that is also assigned to bridge-bound CO.[11] As the pressure is increased further the peak shifts, indicating a decreasing binding energy of CO which could be related to lateral interactions.[12] Similarly, a shoulder on the atop peak appears, that becomes the dominant atop feature at pressures $>2 \times 10^{-2}$ Torr, which could be either related to atop CO populating well-coordinated sites over edge or corner sites,[13] or to local interactions due to a phase transition.[11] At elevated pressures a small feature at 1660 cm^{-1} appears, which we assign to carbonates on the Al$_2$O$_3$.[14]

Generally, the Pd/Al$_2$O$_3$ surface adsorbs CO over a wider set of sites at −93 °C compared to 85 °C. At low temperatures (−93 °C, Fig. 2a) and a CO pressure of 4×10^{-5} Torr two broad and overlapping features are observed centred around 1925 cm^{-1} and 1850 cm^{-1}, that are indicative of CO binding to bridge sites and three-fold hollow sites, respectively. When the pressure is increased to 7×10^{-5} Torr a small feature at $\sim$2060 cm^{-1} appears which is indicative of atop CO. This is similar to RAIRS data on Pd(111) when exposed to 1×10^{-6} Torr CO that exhibits a peak around 2070 cm^{-1} that shifts to 2110 cm^{-1} at temperatures $<$−73 °C.[9,11] As the pressure is further increased to 3×10^{-4} Torr the intensity of the three features increase. From 3×10^{-4} Torr to 1×10^{-2} Torr there is a continual shifting of CO from three-fold sites to bridge-bound sites. Over this pressure range the atop peak broadens *via* an emerging shoulder peak. However, unlike at elevated temperature, the atop peak sharpens as pressure increases and grows to significantly higher relative magnitude. From 1×10^{-2} Torr to 2×10^{-1} Torr the atop peak growth is paired with a loss in magnitude of bridge-bound peaks, suggesting conversion from bridge to atop sites with increasing pressure, similar to work on Pd(111) single crystals.[15]

When comparing the CO adsorption profiles for Pd/Al$_2$O$_3$ at 85 and −93 °C, there are clearly different binding preferences at nearly all pressures. At 85 °C, bridge-bound CO dominates the spectrum at every pressure, and atop CO remains less specifically bound yielding broad features. At −93 °C, bridge-bound CO is only preferred at very low pressures and is converted into

atop configurations as pressure increases. At −93 °C, atop CO may be found in more specific sites because of the sharper features in the DRIFT spectra. This contrasts with non-specific binding for bridge and three-fold binding, as these peaks remain broad and overlapping. For both spectra, no gas phase CO peak is observed. The above results showcase the use of our new vacuum DRIFTS system and method for revealing preferential filling of CO on a Pd/Al$_2$O$_3$ surface, but the resolution provided by this technique is easily expanded to a variety of surfaces and/or combined with other methodologies.

While DRIFTS is a traditionally a steady-state technique, it can be operated under non-steady-state conditions or combined with other transient techniques, such as modulation excitation spectroscopy (MES),[16,17] chemical transient kinetics (CTK),[18,19] and steady-state isotopic transient kinetic analysis (SSITKA).[20] One limitation of transient DRIFTS performed at atmospheric pressure is that the surface can saturate quickly, which limits temporal resolution. By dynamically changing the gas composition behind the leak valve, it is possible to perform transient experiments at reduced pressures significantly increasing temporal resolution while simultaneously ensuring well-defined conditions. During the experiment, the leak valve is opened to the desired pressure and the gas behind the leak valve is dynamically changed either using a switching valve or by modulating the flow rates from the mass flow controllers. Generally, lower total pressure corresponds to higher feature resolution in the transient experiment. However, caution should be taken, particularly at elevated temperatures, to ensure the pressure is high enough to create a representative catalyst surface.

To illustrate transient vacuum DRIFTS, we perform switches between two streams containing either CO or O$_2$ (20% balanced in Ar) at a reactant pressure of 2×10^{-3} Torr at 85 °C (Fig. 3). During the experiments DRIFT spectra were continually acquired $\sim$18 seconds apart while either dosing O$_2$ or CO. First CO was introduced into the DRIFTS cell to saturate the Pd surface, then the gas stream behind the leak valve was switched to O$_2$ to titrate the adsorbed CO* to make CO$_2$ (Fig. 3a). Fig. 3a shows a CO* saturated surface (purple trace) that is subsequently titrated with O$_2$. The CO* peaks lose intensity as O$_2$ is dosed into the cell and titrates away CO* with an initial preference for atop and bridge-bound CO*. As the CO* coverage approximately halves the dominance of bridge-bound CO* is lost. During the course of the titration, we observe the formation of strong carbonate peaks which we assign to adsorption of CO$_2$ to the Al$_2$O$_3$ support.[21] While O* is not visible in the DRIFT spectra, if the pressure is reduced then in-line mass spectrometry can be used to monitor CO$_2$ production to ensure all CO* is titrated away such that O$_2$ can form O* on the surface. Afterwards, the process was performed in reverse, where adsorbed O* was titrated away with CO (Fig. 3b) and the surface then repopulated with CO*. While repopulating the surface with CO*, there is a preference for bridge-bound sites at low coverages, which is opposite to the preference for three-fold hollow sites at low coverages during the O$_2$ titration. Specific peak assignments are outlined in Section S4 and Tables S3, S4 (ESI†).
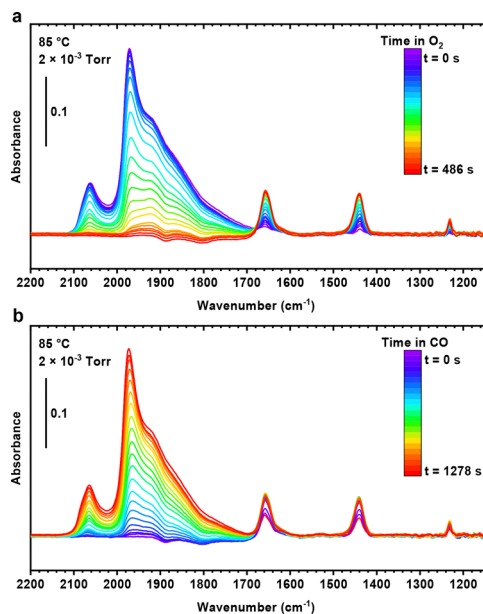
Fig. 3 Time resolved baseline corrected DRIFT spectra during an experiment where (a) adsorbed CO* is titrated using O_2 gas, and (b) where adsorbed O* is titrated using CO gas at 85 °C and a gas phase reactant pressure of 2×10^{-3}. Only select spectra are shown for clarity.

In this communication we demonstrate how to assemble a vacuum DRIFTS cell using readily available components. We report high resolution steady-state and transient DRIFTS measurements of a catalyst surface at pressures from 10^{-5} to 10^{-1} Torr and showcase the preferential filling of binding sites on a Pd/Al_2O_3 catalyst under variable pressures and temperatures. Specifically, we perform measurements that reveal the temperature-dependent preferential adsorption of CO, and how the CO molecules involved in transient CO oxidation have different reactivities based both on adsorption site and the initial state of the catalyst surface. This methodology is broadly applicable and accessible, providing a new simplified method for characterising powdered samples. Thus, we encourage others to adapt their DRIFTS setups to expand their capabilities.

Audrey Dannar: investigation, supervision, writing – original draft, writing – review and editing. Hadley Nunn: investigation, validation, writing – review and editing. Christopher R. O'Connor: conceptualisation, writing – review and editing. Christian Reece: conceptualisation, supervision, writing – review and editing.

Conflicts of interest

There are no conflicts to declare.

Data availability

The data supporting this article have been included as part of the ESI.†

Notes and references

1 R. R. Willey, *App. Spectrosc.*, 1976, **30**, 593–601.
2 M. P. Fuller and P. R. Griffiths, *Anal. Chem.*, 1978, **50**, 1906–1910.
3 F. Zaera, *Chem. Soc. Rev.*, 2014, **43**, 7624–7663.
4 H. Noei, H. Qiu, Y. Wang, E. Löffler, C. Wöll and M. Muhler, *Phys. Chem. Chem. Phys.*, 2008, **10**, 7092–7097.
5 Y. Wang and C. Wöll, *Chem. Soc. Rev.*, 2017, **46**, 1875–1932.
6 E. A. High, E. Lee and C. Reece, *Rev. Sci. Instrum.*, 2023, **94**, 054101.
7 H. Unterhalt, G. Rupprechter and H.-J. Freund, *J. Phys. Chem. B*, 2002, **106**, 356–367.
8 I. V. Yudanov, R. Sahnoun, K. M. Neyman, N. Rösch, J. Hoffmann, S. Schauermann, V. Johánek, H. Unterhalt, G. Rupprechter, J. Libuda and H.-J. Freund, *J. Phys. Chem. B*, 2003, **107**, 255–264.
9 W. K. Kuhn, J. Szanyi and D. W. Goodman, *Surf. Sci.*, 1992, **274**, L611–L618.
10 E. Ozensoy, D. C. Meier and D. W. Goodman, *J. Phys. Chem. B*, 2002, **106**, 9367–9371.
11 D. R. Rainer, M.-C. Wu, D. I. Mahon and D. W. Goodman, *J. Vacuum Sci. Technol. A*, 1996, **14**, 1184–1188.
12 A. M. Bradshaw and F. M. Hoffmann, *Surf. Sci.*, 1978, **72**, 513–535.
13 D. Gun Oh, H. A. Aleksandrov, H. Kim, I. Z. Koleva, K. Khivantsev, G. N. Vayssilov and J. Hun Kwak, *Chem. – Eur. J.*, 2022, **28**, e202200684.
14 C. Weilach, C. Spiel, K. Föttinger and G. Rupprechter, *Surf. Sci.*, 2011, **605**, 1503–1509.
15 W. K. Kuhn, J. Szanyi and D. W. Goodman, *Surf. Sci.*, 1992, **274**, L611–L618.
16 J. Weyel, L. Schumacher, M. Ziemba, M. Pfeiffer and C. Hess, *Acc. Chem. Res.*, 2024, **57**, 2643–2652.
17 P. Müller and I. Hermans, *Ind. Eng. Chem. Res.*, 2017, **56**, 1123–1136.
18 A. Raub, H. Karroum, M. Athariboroujeny and N. Kruse, *Catal. Lett.*, 2021, **151**, 613–626.
19 A. Frennet and C. Hubert, *J. Mol. Catal. A: Chem.*, 2000, **163**, 163–188.
20 T. Otroshchenko, V. A. Kondratenko, A. Zanina, Q. Zhang and E. V. Kondratenko, *ChemCatChem*, 2024, **16**, e202400081.
21 K. Föttinger, W. Emhofer, D. Lennon and G. Rupprechter, *Top. Catal.*, 2017, **60**, 1722–1734.